Optimal position and velocity navigation filters for autonomous vehicles

Pedro Batista, Carlos Silvestre, and Paulo Oliveira

Automatica, vol. 46, no. 4, pp. 767-774, April 2010

https://doi.org/10.1016/j.automatica.2010.02.004

Optimal Position and Velocity Navigation Filters for Autonomous Vehicles ⋆

Pedro Batista [2] Carlos Silvestre Paulo Oliveira

Instituto Superior Técnico, Institute for Systems and Robotics
Av. Rovisco Pais, 1049-001 Lisboa, Portugal

Abstract

This paper presents the design and performance evaluation of a set of globally stable time-varying kinematic filters with application to the estimation of linear motion quantities of mobile platforms (position, linear velocity, and acceleration) in three dimensions. The proposed techniques are based on the Kalman and $\mathcal{H}_\infty$ optimal filters for linear time-varying systems and the explicit optimal filtering solutions are obtained through the use of an appropriate coordinate transformation, whereas the design employs frequency weights to achieve adequate disturbance rejection and attenuation of the measurement noise on the state estimates. Two examples of application in the field of ocean robotics are presented that demonstrate the potential and usefulness of the proposed design methodology. In the first the proposed filtering solutions allow for the design of a complementary navigation filter for the estimation of unknown constant ocean currents, while the second addresses the problem of estimation of the velocity of an underwater vehicle, as well as the acceleration of gravity. Simulation results are included that illustrate the filtering achievable performance in the presence of both extreme environmental disturbances and realistic measurement noise.

Key words: Underwater vehicles; navigation; mobile robots; autonomous systems; estimation theory.

1. Introduction

Navigation and Positioning Systems play a key role in the development of a large variety of mobile platforms for land, air, space, and marine applications. In the domain of marine research, for instance, the quality of the navigation data is a fundamental requirement in applications that range from ocean sonar surveying to ocean data acquisition or sample collection, as the acquired data sets should be properly geo-referenced with respect to a given mission reference point. For control purposes other quantities such as the attitude of the vehicle and/or the linear and angular velocities are also commonly required. This paper presents a set of optimal time-varying filtering solutions for a class of kinematic systems with direct application to the estimation of linear motion quantities in accurate Integrated Navigation Systems.

To tackle this class of problems several approaches have been proposed in the literature. In [7] a globally exponentially stable (GES) nonlinear control law is presented for ships, in two-dimensions, which includes a nonlinear observer to provide the state of the vehicle. This observer relies on the vehicle dynamics but, as discussed in [14], it does not apply to unstable ships. In the latter a solution to an extended class of ships is proposed requiring only stable surge dynamics. In [6] a GES observer for ships (in two-dimensions) that includes features such as wave filtering and bias estimation is presented and in [8] an extension to this result with adaptive wave filtering is available. An alternative filter was proposed in [12] where the problem of estimating the velocity and position of an autonomous vehicle in three-dimensions was solved by resorting to special bilinear time-varying complementary filters. More recently, a pair of coworking nonlinear Luenberger GES observers for autonomous underwater vehicles (AUVs), in 3D, was proposed in [13], which also elaborates on the destabilizing Coriolis and centripetal forces and moments. However, this last approach assumes, among others, limited pitch angles. A more complete survey on the subject of underwater vehicle navigation can be found in [9]. General drawbacks of the above-mentioned results include the absence of systematic tuning procedures and the inherent limitations of the vehi-

⋆ This paper was not presented at any IFAC meeting.

[1] This work was partially supported by Fundação para a Ciência e a Tecnologia (ISR/IST plurianual funding) and project MEDIRES from ADI through the POS_Conhecimento Program that includes FEDER funds, and by the project PDCT/MAR/55609/2004 - RUMOS of the FCT.

[2] The work of P. Batista was supported by a PhD Student Scholarship from the POCTI Programme of FCT, SFRH/BD/24862/2005.
Corresponding author. Tel.: +351 218418054; fax:+351 218418291

cle dynamic models, which are seldom known in full detail and may be subject to variations over time. Previous work by the authors can be found in [4].

The main contribution of this paper is a new filtering design methodology for a class of kinematic systems with application to the estimation of linear quantities (position, linear velocity, ocean current, and gravity acceleration) in Integrated Navigation Systems that

(i) presents globally exponentially stable error dynamics which are also globally input-to-state stable (ISS) with respect to disturbances on the key quantities;
(ii) is optimal with respect to disturbances arising from all sensors but the Attitude and Heading Reference System (AHRS);
(iii) provides a systematic design procedure based upon well known filtering results, that allows for the use of frequency weights to shape the dynamic response of the filter;
(iv) includes a limit filtering solution that is computationally efficient and therefore appropriate for implementation in low-cost, low-power hardware.

The methodology proposed in this paper relies on the design of optimal time-varying Navigation filters based on the steady-state Kalman and $\mathcal{H}_\infty$ filter solutions for equivalent linear time invariant (LTI) systems. This equivalence is established through a time-varying orthogonal coordinate transformation that is readily available from an AHRS. An example of previous use of Lyapunov transformations in the design of estimators can be found in [11]. Applications of the proposed filter design techniques are presented to estimate linear quantities in Integrated Navigation Systems for mobile platforms. To describe the vehicle tri-dimensional motion the proposed filters rely on pure kinematic models. This class of models, expressed in the inertial coordinate system, has been widely used by the Navigation community, see [15] and references therein. The present solution departs from previous approaches as it considers the rigid-body kinematics expressed in body-fixed coordinates, thus avoiding the algebraic transformation of sensor data to inertial coordinates, which is strongly undesirable since the effect of the noise on the attitude may be greatly amplified on the state estimates.

The paper is organized as follows. The motivation behind the work is presented in Section 2, whereas the theoretical background that supports the navigation solutions proposed in the paper is presented in Section 3. Simulation results are included, in Section 4, that illustrate the achievable performance of the proposed solutions in the presence of extreme environmental disturbances and realistic measurement noise. Finally, Section 5 summarizes the main contributions of the paper.

Notation and definitions: Throughout the paper the symbol $\mathbf{0}_{n\times m}$ denotes an $n \times m$ matrix of zeros, $\mathbf{I}_n$ an identity matrix with dimension $n \times n$, and $\mathrm{diag}(\mathbf{A}_1, \ldots, \mathbf{A}_n)$ a block diagonal matrix. When omitted the matrices are assumed of appropriate dimensions. The Special Orthogonal Group $\left\{\mathbf{R} \in \mathbb{R}^{3\times 3} : \ \mathbf{R}^T\mathbf{R} = \mathbf{I}_3, \ \det(\mathbf{R}) = 1\right\}$ is denoted by $SO(3)$ and the usual Hilbert space of square integrable functions is denoted by $\mathcal{L}_2$.

2. Motivation

2.1. *Position and ocean current estimation*

The first example provided in this section revisits the problem originally described in [3]. Consider an underwater vehicle equipped with an acoustic positioning system like an Ultra-Short Baseline (USBL) positioning sensor and suppose that there is a moored buoy in the mission scenario where an acoustic transponder is installed. The position of the transponder with respect to the vehicle is available, in body-fixed coordinates, as measured by the USBL sensor installed on-board. The linear motion kinematics of the vehicle are given by $\dot{\mathbf{p}}(t) = \mathbf{R}(t)\mathbf{v}(t)$, where $\mathbf{p} \in \mathbb{R}^3$ is the position of the origin of the body-fixed coordinate system $\{B\}$ described in the inertial coordinate system $\{I\}$, $\mathbf{R} \in SO(3)$ is the rotation matrix from $\{B\}$ to $\{I\}$, that verifies

$$\dot{\mathbf{R}}(t) = \mathbf{R}(t)\mathbf{S}\left(\boldsymbol{\omega}(t)\right), \tag{1}$$

where $\mathbf{S}(\boldsymbol{\omega}(t)) \in \mathbb{R}^{3\times 3}$ is a skew-symmetric matrix that verifies $\mathbf{S}(\mathbf{a})\,\mathbf{b} = \mathbf{a} \times \mathbf{b}$, with $\times$ denoting the cross product, $\boldsymbol{\omega} \in \mathbb{R}^{3\times 3}$ is the vehicle angular velocity, expressed in body-fixed coordinates, and $\mathbf{v} \in \mathbb{R}^{3\times 3}$ is the linear velocity of the vehicle relative to $\{I\}$, also expressed in body-fixed coordinates. An Attitude and Heading Reference System (AHRS) provides the body angular velocity $\boldsymbol{\omega}$ and the rotation matrix $\mathbf{R}$. Finally, suppose that the vehicle is moving in deep waters (far from the wave action), in the presence of an ocean current of constant velocity, which expressed in body-fixed coordinates is represented by $\mathbf{v}_c$. In addition to that, assume that the buoy where the transponder is installed is subject to wave action of known power spectral density that affects its position over time. The problem considered here is that of estimate the velocity of the current and the position of the transponder with respect to the vehicle, filtering the disturbances induced by the waves. Further consider that the velocity of the vehicle relative to the water is available from the measures of an on-board Doppler velocity log (DVL). In shallow waters, this sensor can be employed to measure both the velocity of the vehicle relative to the inertial frame and relative to the water. However, when the vehicle is far from the seabed the inertial velocity is usually unavailable. By estimating the ocean current velocity, an estimate of the velocity of the vehicle relative to the inertial frame is immediately obtained.

Let $\mathbf{e} \in \mathbb{R}^3$ denote the position of the transponder relative to the vehicle and $\mathbf{v}_r \in \mathbb{R}^3$ denote the velocity of the vehicle relative to the fluid, both expressed in body-fixed coordinates. Since the transponder is assumed at rest in the inertial frame (in the absence of environmental disturbances), the time derivative of $\mathbf{e}$ is given by

$$\dot{\mathbf{e}}(t) = -\mathbf{v}_r(t) - \mathbf{v}_c(t) - \mathbf{S}\left(\boldsymbol{\omega}(t)\right)\mathbf{e}(t). \tag{2}$$

On the other hand, since the velocity of the fluid is assumed to be constant in the inertial frame, the time derivative of this quantity expressed in body-fixed coordinates is simply given by

$$\dot{\mathbf{v}}_c(t) = -\mathbf{S}\left(\boldsymbol{\omega}(t)\right)\mathbf{v}_c(t). \tag{3}$$

The problem considered here is the design of a filter for the nominal system (2)-(3), considering also the rejection of eventual system disturbances and sensor noise.

2.2. *Position, velocity, and gravity estimation*

The solution for the problem presented in the previous section also yields an estimate of the velocity of the vehicle indirectly, as $\mathbf{v} = \mathbf{v}_r + \mathbf{v}_c$. The bottleneck is that the noise of the relative velocity measurements appears directly in the inertial velocity estimate. To avoid that, consider a similar setup, where a vehicle is moving in a similar mission scenario equipped with an USBL, that provides $\mathbf{e}$, an AHRS, which gives both $\boldsymbol{\omega}$ and $\mathbf{R}$, and an accelerometer instead of a Doppler Velocity Log. The acceleration measurements satisfy

$$\mathbf{a}(t) = \dot{\mathbf{v}}(t) - \mathbf{g}(t) + \mathbf{S}\left(\boldsymbol{\omega}(t)\right)\mathbf{v}(t), \tag{4}$$

where $\mathbf{a} \in \mathbb{R}^3$ is the accelerometer measurement and $\mathbf{g} \in \mathbb{R}^3$ denotes the gravity acceleration vector expressed in body-fixed coordinates. The problem here considered is that of estimate the linear position of the vehicle with respect to the undisturbed position of the transponder, the linear velocity of the vehicle relative to the inertial frame, and the gravity acceleration vector, all expressed in body-fixed coordinates. This last point is of major importance in the design of Navigation Systems as, due to its magnitude, any misalignment in the estimation of the gravity acceleration vector results in severe problems in the acceleration compensation.

The time derivative of $\mathbf{e}$, given by (2), can be rewritten, in order to fit in the dynamics of this new sensor suite, as

$$\dot{\mathbf{e}}(t) = -\mathbf{v}(t) - \mathbf{S}\left(\boldsymbol{\omega}(t)\right)\mathbf{e}(t). \tag{5}$$

On the other hand, from (4) it follows that

$$\dot{\mathbf{v}}(t) = \mathbf{a}(t) + \mathbf{g}(t) - \mathbf{S}\left(\boldsymbol{\omega}(t)\right)\mathbf{v}(t). \tag{6}$$

Assuming the gravity acceleration vector constant in the inertial frame its time derivative in body frame coordinates can be written as

$$\dot{\mathbf{g}}(t) = -\mathbf{S}\left(\boldsymbol{\omega}(t)\right)\mathbf{g}(t). \tag{7}$$

The problem considered here is that of the designing a filter for the nominal system dynamics (5)-(7), considering also the rejection of system disturbances and sensor noise.

3. Filter Design

This section presents the kinematic filter design methodologies that support the navigation solutions proposed in the paper. The class of system dynamics is introduced in Section 3.1, whereas the Kalman filter for such systems is derived in Section 3.2. The $\mathcal{H}_\infty$ optimal filter is presented in Section 3.3 and finally some properties and alternative solutions are discussed in Section 3.4.

3.1. *System dynamics*

Consider the class of dynamic systems

$$\begin{cases} \dot{\boldsymbol{\eta}}_p(t) = \mathbf{A}_p\boldsymbol{\eta}_p(t) - \mathbf{M}_S(\boldsymbol{\omega}(t))\boldsymbol{\eta}_p(t) + \mathbf{B}_p(t)\mathbf{u}(t) + \mathbf{T}^T(t)\mathbf{d}(t) \\ \boldsymbol{\psi}(t) = \boldsymbol{C}_p\boldsymbol{\eta}_p(t) + \mathbf{R}^T(t)\mathbf{n}(t) \end{cases}, \tag{8}$$

where $\boldsymbol{\eta}_p(t) = \left[\boldsymbol{\eta}_1^T(t) \ \dots \ \boldsymbol{\eta}_N^T(t)\right]^T$, with $\boldsymbol{\eta}_i(t) \in \mathbb{R}^3$, $i = 1, \dots, N$, is the system state, $\boldsymbol{\psi}(t) \in \mathbb{R}^3$ is the system output, $\mathbf{u}(t)$ is a deterministic system input, $\boldsymbol{\omega}(t) \in \mathbb{R}^3$ is a continuous bounded function of t, $\mathbf{d}(t) \in \mathbb{R}^{3N}$ denotes the system disturbances input, $\mathbf{n}(t) \in \mathbb{R}^3$ denotes the noise of the sensors, $\mathbf{T}(t) := \mathrm{diag}\left(\mathbf{R}(\mathrm{t}), \dots, \mathbf{R}(\mathrm{t})\right) \in \mathbb{R}^{3\mathrm{N}\times 3\mathrm{N}}$, where $\mathbf{R}(t) \in SO(3)$ is a proper rotation matrix, as previously defined, that satisfies (1), $\mathbf{M}_S\left(\boldsymbol{\omega}(t)\right)$ is the block diagonal matrix

$$\mathbf{M}_S\left(\boldsymbol{\omega}(t)\right) := \mathrm{diag}\left(\mathbf{S}(\boldsymbol{\omega}(t)), \ \dots, \ \mathbf{S}(\boldsymbol{\omega}(t))\right) \in \mathbb{R}^{3N\times 3N},$$

$$\mathbf{A}_p = \begin{bmatrix} \mathbf{0} & \gamma_1\mathbf{I}_3 & \mathbf{0} & \dots & \mathbf{0} \\ \vdots & \ddots & \ddots & \ddots & \vdots \\ \vdots & & \ddots & \ddots & \mathbf{0} \\ \vdots & & & \ddots & \gamma_{N-1}\mathbf{I}_3 \\ \mathbf{0} & \dots & \dots & \dots & \mathbf{0} \end{bmatrix} \in \mathbb{R}^{3N\times 3N}, \ \gamma_i \in \mathbb{R},$$

where $\gamma_i \neq 0$, $i = 1, \dots, N-1$, $\mathbf{B}_p(t)$ is a generic system input matrix, of appropriate dimensions, and $\mathbf{C}_p = [\mathbf{I}_3 \, \mathbf{0}_{3\times 3} \ \dots \ \mathbf{0}_{3\times 3}] \in \mathbb{R}^{3\times 3N}$. It is assumed that $\mathbf{R}(t)$ and $\boldsymbol{\omega}(t)$ are known over time. Notice that the disturbance input $\mathbf{d}$ and the noise of the sensors $\mathbf{n}$ affect the state and the system output through time-varying transformations, $\mathbf{T}(t)$ and $\mathbf{R}(t)$, respectively. Nevertheless, these transformations preserve the norm of the disturbances and the noise of the sensors - only the directionality is affected over time. It is easy to see that both system dynamics (2)-(3) and (5)-(7) fit in the class of systems (8).

For design purposes, consider the augmented plant as depicted in Fig. 1. In the figure, $\mathbf{w}_d$ and $\mathbf{w}_n$ represent generalized disturbance vectors and $\mathcal{W}_d$ and $\mathcal{W}_n$ are linear time invariant filters included to shape both the noise of the sensors $\mathbf{n}$ and the state disturbances $\mathbf{d}$, see [2] for details on the use of pre-filters to model colored noise. The assumptions on $\mathbf{w}_d$ and $\mathbf{w}_n$, that drive the filters $\mathcal{W}_d$ and $\mathcal{W}_n$, respectively, depend on the particular filter design and are presented in the sequel.

Let $\mathbf{w}(t) := \left[\mathbf{w}_d^T(t) \, \mathbf{w}_n^T(t)\right]^T$ and define the augmented state vector $\boldsymbol{\eta}(t) := \left[\boldsymbol{\eta}_p^T(t) \, \mathbf{x}_d^T(t) \, \mathbf{x}_n^T(t)\right]^T$, where $\mathbf{x}_d$ and $\mathbf{x}_n$ denote the states of the state space realizations $(\mathbf{A}_d, \mathbf{B}_d, \mathbf{C}_d, \mathbf{D}_d)$ and $(\mathbf{A}_n, \mathbf{B}_n, \mathbf{C}_n, \mathbf{D}_n)$ of the filters $\mathcal{W}_d$

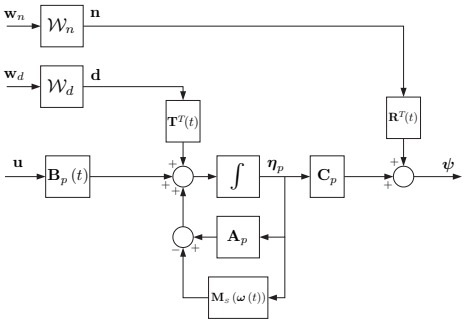

Fig. 1. Generalized design framework

and $\mathcal{W}_n$, respectively. The augmented dynamics corresponding to the generalized design framework, depicted in Fig. 1, can be written as

$$\begin{cases} \dot{\boldsymbol{\eta}}(t) = \boldsymbol{\mathcal{A}}(t)\boldsymbol{\eta}(t) + \boldsymbol{\mathcal{B}}_p(t)\mathbf{u}(t) + \boldsymbol{\mathcal{B}}(t)\mathbf{w}(t) \\ \boldsymbol{\psi}(t) = \boldsymbol{\mathcal{C}}(t)\boldsymbol{\eta}(t) + \boldsymbol{\mathcal{D}}(t)\mathbf{w}(t) \end{cases}, \tag{9}$$

where

$$\boldsymbol{\mathcal{A}}(t) = \begin{bmatrix} \mathbf{A}_p - \mathbf{M}_S(\boldsymbol{\omega}(t)) & \mathbf{T}^T(t)\mathbf{C}_d & \mathbf{0} \\ \mathbf{0} & \mathbf{A}_d & \mathbf{0} \\ \mathbf{0} & \mathbf{0} & \mathbf{A}_n \end{bmatrix},$$

$$\boldsymbol{\mathcal{B}}_p(t) = \begin{bmatrix} \mathbf{B}_p(t) \\ \mathbf{0} \\ \mathbf{0} \end{bmatrix}, \boldsymbol{\mathcal{B}}(t) := \begin{bmatrix} \mathbf{T}^T(t)\mathbf{D}_d & \mathbf{0} \\ \mathbf{B}_d & \mathbf{0} \\ \mathbf{0} & \mathbf{B}_n \end{bmatrix},$$

$\boldsymbol{\mathcal{C}}(t) = \begin{bmatrix} \mathbf{C}_p \,|\, \mathbf{0} \,|\, \mathbf{R}^T(t)\mathbf{C}_n \end{bmatrix}$, and $\boldsymbol{\mathcal{D}}(t) = \begin{bmatrix} \mathbf{0} \mid \mathbf{R}^T(t)\mathbf{D}_n \end{bmatrix}$.

3.2. *Kalman filter*

This section presents the derivation of the time-varying Kalman filter for the dynamic system (8) subject to system disturbances and measurement noise. The main idea, which is also at the core of the $\mathcal{H}_\infty$ filter design, consists of converting the linear time-varying dynamic system into an equivalent LTI system. A classic Kalman filter is then applied to the resulting LTI system and the explicit optimal solution in the original state space is obtained by reversing the previous coordinate transformation. In this section the generalized disturbance vector $\mathbf{w}$ is assumed to be continuous-time zero-mean unit intensity white Gaussian noise.

Without loss of generality, consider the dynamic system (8) without the deterministic input $\mathbf{u}(t)$ and define $\mathbf{x}(t) = \begin{bmatrix} \mathbf{x}_p(t)^T \, \mathbf{x}_d(t)^T \, \mathbf{x}_n(t)^T \end{bmatrix}^T$ as

$$\mathbf{x}(t) := \mathbf{T}_c(t)\boldsymbol{\eta}(t), \tag{10}$$

where $\mathbf{T}_c(t)$ is the transformation matrix defined by

$$\mathbf{T}_c(t) := \operatorname{diag}\left(\mathbf{T}(\mathrm{t}),\, \mathbf{I},\, \mathbf{I}\right).$$

Notice that (10) is a Lyapunov transformation (see [5]) since $\mathbf{T}(t)$ is continuous differentiable for all t, $\mathbf{T}(t)$ and $\dot{\mathbf{T}}(t)$ are bounded for all t, where $\dot{\mathbf{T}}(t) = \mathbf{T}(t)\mathbf{M}_S(\boldsymbol{\omega}(t))$, and $\det\left[\mathbf{T}(t)\right] = 1$. Therefore, all stability, observability, and controllability properties are preserved. Define also a new equivalent system output as

$$\mathbf{y}(t) := \mathbf{R}(t)\boldsymbol{\psi}(t).$$

It is straightforward to show that after these coordinate transformations the resulting system dynamics are LTI, given by

$$\begin{cases} \dot{\mathbf{x}}(t) = \mathbf{A}\mathbf{x}(t) + \mathbf{B}\mathbf{w}(t) \\ \mathbf{y}(t) = \mathbf{C}\mathbf{x}(t) + \mathbf{D}\mathbf{w}(t) \end{cases},$$

where

$$\mathbf{A} := \begin{bmatrix} \mathbf{A}_p & \mathbf{C}_d & \mathbf{0} \\ \mathbf{0} & \mathbf{A}_d & \mathbf{0} \\ \mathbf{0} & \mathbf{0} & \mathbf{A}_n \end{bmatrix}, \quad \mathbf{B} := \begin{bmatrix} \mathbf{D}_d & \mathbf{0} \\ \mathbf{B}_d & \mathbf{0} \\ \mathbf{0} & \mathbf{B}_n \end{bmatrix},$$

$\mathbf{C} = [\mathbf{C}_p \; \mathbf{0} \; \mathbf{C}_n]$, and $\mathbf{D} = [\mathbf{0} \; \mathbf{D}_n]$. It is assumed that the Kalman filtering problem is well-posed (this only depends, in this case, on the choice of the frequency weights, as the nominal system is observable). Define $\mathbf{V}$ as

$$\mathbf{V} := \begin{bmatrix} \mathbf{B} \\ \mathbf{D} \end{bmatrix} \begin{bmatrix} \mathbf{B}^T \, \mathbf{D}^T \end{bmatrix} = \begin{bmatrix} \mathbf{V}_{xx} & \mathbf{V}_{xy} \\ \mathbf{V}_{xy}^T & \mathbf{V}_{yy} \end{bmatrix}.$$

The Kalman filter for this system is given by (see [1] [2])

$$\dot{\hat{\mathbf{x}}}(t) = \mathbf{A}\hat{\mathbf{x}}(t) + \mathbf{K}_2(t)\left[\mathbf{y}(t) - \mathbf{C}\hat{\mathbf{x}}(t)\right],$$

where $\mathbf{K}_2(t)$ is the Kalman gain matrix, given by

$$\mathbf{K}_2(t) = \left[\mathbf{P}_2(t)\mathbf{C}^T + \mathbf{V}_{xy}\right]\mathbf{V}_{yy}^{-1},$$

where $\mathbf{P}_2(t)$ is the solution of the matrix differential Riccati equation

$$\begin{aligned} \dot{\mathbf{P}}_2(t) = {} & \mathbf{A}_e\mathbf{P}_2(t) + \mathbf{P}_2(t)\mathbf{A}_e^T - \mathbf{P}_2(t)\mathbf{C}^T\mathbf{V}_{yy}^{-1}\mathbf{C}\mathbf{P}_2(t) \\ & + \mathbf{V}_{xx} - \mathbf{V}_{xy}\mathbf{V}_{yy}^{-1}\mathbf{V}_{xy}^T, \end{aligned} \tag{11}$$

with $\mathbf{A}_e = \mathbf{A} - \mathbf{V}_{xy}\mathbf{V}_{yy}^{-1}\mathbf{C}$. The initial condition $\mathbf{P}_2\left(t_0\right)$ will be given in the sequel.

In order to recover the filter equations in the appropriate coordinate space, consider the inverse coordinate transformation

$$\hat{\boldsymbol{\eta}}(t) = \mathbf{T}_c^T(t)\hat{\mathbf{x}}(t). \tag{12}$$

The time derivative of (12) yields the final filter equations

$$\dot{\hat{\boldsymbol{\eta}}}(t) = \boldsymbol{\mathcal{A}}(t)\hat{\boldsymbol{\eta}}(t) + \boldsymbol{\mathcal{B}}_p(t)\mathbf{u}(t) + \boldsymbol{\mathcal{K}}_2(t)\left[\boldsymbol{\psi}(t) - \boldsymbol{\mathcal{C}}(t)\hat{\boldsymbol{\eta}}(t)\right], \tag{13}$$

where the Kalman gain is given by

$$\boldsymbol{\mathcal{K}}_2(t) = \mathbf{T}_c^T(t)\mathbf{K}_2(t)\mathbf{R}(t). \tag{14}$$

Notice that the deterministic input term $\boldsymbol{\mathcal{B}}_p(t)\mathbf{u}(t)$ was included to complete the filter dynamics.

The following lemma is the main result of this section.

Lemma 1 *Consider the generalized system dynamics* (9)*, where* $\mathbf{w}$ *is continuous-time zero-mean unit intensity white Gaussian noise. Let* $\boldsymbol{\mathcal{P}}_0$ *be the initial error covariance matrix*

of the system state estimate $\hat{\boldsymbol{\eta}}$. Then, the Kalman filter is given by (13)*, where the initial condition for the differential equation* (11) *is* $\mathbf{P}_2(t_0) = \mathbf{T}_c(t_0)\boldsymbol{\mathcal{P}}_0\mathbf{T}_c^T(t_0)$.

PROOF. The Kalman filter has the structure of (13) and it is a simple matter to show that the corresponding covariance matrix may be written as $\boldsymbol{\mathcal{P}}_2(t) := \mathbf{T}_c^T(t)\mathbf{P}_2(t)\mathbf{T}_c(t)$. From that it follows that the Kalman gain may be expressed as in (14), which concludes the proof.

3.3. $\mathcal{H}_\infty$ *optimal filter*

The Kalman filter is the optimal filtering solution for a particular case of system disturbances and measurement noise. However, it is often the case that the noise distributions are unknown or do not satisfy the assumptions of Lemma 1. This section introduces the $\mathcal{H}_\infty$ optimal filter for the class of dynamic systems (9), which deals with worst case scenarios.

The $\mathcal{H}_\infty$ filtering framework is quite similar to the one presented in Fig. 1. The difference is that the generalized disturbance vector $\mathbf{w}(t)$ is, in this case, assumed to be square integrable, i.e., $\mathbf{w} \in \mathcal{L}_2$. Moreover, an additional performance variable is defined as

$$\boldsymbol{\zeta}(t) := \mathbf{L}_\infty\mathbf{T}(t)\boldsymbol{\eta}_p = \boldsymbol{\mathcal{L}}(t)\boldsymbol{\eta},$$

with $\boldsymbol{\mathcal{L}}(t) := \mathbf{L}\mathbf{T}_c(t)$, $\mathbf{L} := [\mathbf{L}_\infty\ \mathbf{0}\,\mathbf{0}]$, where $\mathbf{L}_\infty$ is a matrix that weights the different states. The goal is to design a filter to obtain an estimate $\hat{\boldsymbol{\zeta}}(t)$ of $\boldsymbol{\zeta}(t)$, using the output $\boldsymbol{\psi}(t)$, that minimizes

$$J_\infty := \sup_{\mathbf{0}\neq(\boldsymbol{\eta}_0,\mathbf{w})\in\mathbb{R}^{3N}\times\mathcal{L}_2} \frac{\left\|\boldsymbol{\zeta}-\hat{\boldsymbol{\zeta}}\right\|^2}{\|\mathbf{w}\|^2 + \boldsymbol{\eta}_0^T\mathbf{R}_0\boldsymbol{\eta}_0},$$

with $\boldsymbol{\eta}(t_0) = \boldsymbol{\eta}_0$, $\mathbf{R}_0 = \mathbf{R}_0^T \succ \mathbf{0}$.

The solution to this problem is well known (see [10]) and, as the design follows similar steps as for the Kalman filter, previously derived in detail, only the final result is summarized in the next lemma.

Lemma 2 *Consider the generalized dynamics presented in Fig. 1, where* $\mathbf{w}_d, \mathbf{w}_n \in \mathcal{L}_2$*. There exists a filter such that* $J_\infty < \gamma^2$ *if and only if there exits a symmetric positive definite matrix* $\mathbf{P}_\infty(t)$ *that satisfies*

$$\begin{aligned}\dot{\mathbf{P}}_\infty(t) &= \mathbf{A}_e\mathbf{P}_\infty(t) + \mathbf{P}_\infty(t)\mathbf{A}_e^T - \mathbf{P}_\infty(t)\mathbf{C}^T\mathbf{V}_{yy}^{-1}\mathbf{C}\mathbf{P}_\infty(t)\\ &\quad+\frac{1}{\gamma^2}\mathbf{P}_\infty(t)\mathbf{L}^T\mathbf{L}\mathbf{P}_\infty(t) + \mathbf{V}_{xx} - \mathbf{V}_{xy}\mathbf{V}_{yy}^{-1}\mathbf{V}_{xy}^T, \quad (15)\end{aligned}$$

with $\mathbf{P}_\infty(t_0) = \mathbf{T}_c(t_0)\mathbf{R}_0^{-1}\mathbf{T}_c^T(t_0)$*, and such that the unforced linear time-varying system*

$$\dot{\mathbf{p}}_\infty(t) = \left[\mathbf{A}_e - \mathbf{P}_\infty(t)\left(\mathbf{C}^T\mathbf{V}_{yy}^{-1}\mathbf{C} - \frac{1}{\gamma^2}\mathbf{L}^T\mathbf{L}\right)\right]\mathbf{p}_\infty(t) \quad (16)$$

is exponentially stable. Moreover, the filter structure is equal to the structure of the Kalman filter, with gain

$$\boldsymbol{\mathcal{K}}_\infty(t) = \left[\boldsymbol{\mathcal{P}}_\infty(t)\boldsymbol{\mathcal{C}}^T(t) + \boldsymbol{\mathcal{V}}_{xy}(t)\right]\boldsymbol{\mathcal{V}}_{yy}^{-1}(t),$$

where

$$\boldsymbol{\mathcal{P}}_\infty(t) = \mathbf{T}_c^T(t)\mathbf{P}_\infty(t)\mathbf{T}_c(t). \quad (17)$$

PROOF. It is straightforward to show that (17) is the solution of the corresponding $\mathcal{H}_\infty$ differential Riccati equation, with $\boldsymbol{\mathcal{P}}_\infty(t_0) = \mathbf{R}_0^{-1}$. Moreover, if the LTV system (16) is exponentially stable, so is the LTV unforced system

$$\dot{p}_\infty(t) = \left[\boldsymbol{\mathcal{A}}_e(t) - \boldsymbol{\mathcal{P}}_\infty(t)\left(\boldsymbol{\mathcal{C}}^T(t)\boldsymbol{\mathcal{V}}_{yy}^{-1}(t)\boldsymbol{\mathcal{C}}(t) - \frac{1}{\gamma^2}\boldsymbol{\mathcal{L}}^T(t)\boldsymbol{\mathcal{L}}(t)\right)\right]p_\infty(t),$$

as $p_\infty(t) = \mathbf{T}_c^T(t)\mathbf{p}_\infty(t)$, which is a Lyapunov transformation (see [5]). This suffices to complete the proof, see [10].

Remark 1 *If* $\mathbf{L}$ *commutes with* $\mathbf{T}(t)$*, then the* $\mathcal{H}_\infty$ *performance variable can be rewritten as* $\boldsymbol{\zeta}(t) = \mathbf{L}\boldsymbol{\eta}_p(t)$*, which weights directly the system states. This is often the case, e.g., when* $\mathbf{L}$ *is of the form* $\mathbf{L} = [l_1\mathbf{I}_3\ \ldots\ l_N\mathbf{I}_3]$*,* $l_i \in \mathbb{R}$*,* $i = 1, \ldots, N$*.*

3.4. *Filter properties and extensions*

3.4.1. *Limit Filtering Solutions*

The proposed Kalman filter gain matrix $\boldsymbol{\mathcal{K}}_2(t)$ has a limit solution, although the system at hand is not LTI. Indeed, as t approaches infinity, $\mathbf{P}_2(t)$ converges to the solution $\mathbf{P}_2^\infty$ of the algebraic Riccati equation

$$\mathbf{A}_e\mathbf{P}_2^\infty + \mathbf{P}_2^\infty\mathbf{A}_e^T - \mathbf{P}_2^\infty\mathbf{C}^T\mathbf{V}_{yy}^{-1}\mathbf{C}\mathbf{P}_2^\infty + \mathbf{V}_{xx} - \mathbf{V}_{xy}\mathbf{V}_{yy}^{-1}\mathbf{V}_{xy}^T = \mathbf{0}.$$

Thus, as t approaches infinity, $\mathbf{K}_2(t)$ converges to $\mathbf{K}_2^\infty := \left[\mathbf{P}_2^\infty\mathbf{C}^T + \mathbf{V}_{xy}\right]\mathbf{V}_{yy}^{-1}$ and therefore

$$\lim_{t\to\infty}\left\|\boldsymbol{\mathcal{K}}_2(t) - \mathbf{T}_c^T(t)\mathbf{K}_2^\infty\mathbf{R}(t)\right\| = \mathbf{0}.$$

This is a fundamental property in practical applications, as the filter gain can be replaced by the corresponding limit solution, $\mathbf{T}_c^T(t)\mathbf{K}_2^\infty\mathbf{R}(t)$, of which $\mathbf{K}_2^\infty$ can be easily obtained offline from the solution of an algebraic Riccati equation.

As with the Kalman filter, the $\mathcal{H}_\infty$ optimal filter also achieves a limit solution. Indeed, as discussed in [10], as t approaches infinity, $\mathbf{P}_\infty(t)$ converges to the solution $\mathbf{P}_\infty^\infty$ of the corresponding $\mathcal{H}_\infty$ matrix algebraic Riccati equation, with $\dot{\mathbf{P}}_\infty(t) = \mathbf{0}$ in (15). Thus,

$$\lim_{t\to\infty}\left\|\boldsymbol{\mathcal{P}}_\infty(t) - \mathbf{T}_c^T(t)\mathbf{P}_\infty^\infty\mathbf{T}_c(t)\right\| = \mathbf{0}$$

and the filter asymptotically converges to the corresponding linear time-varying filter that is obtained from the linear time invariant $\mathcal{H}_\infty$ filtering solution when the initial condition is known.

3.4.2. *Effect of perturbations in* $\mathbf{R}(t)$ *and* $\mathbf{S}(\boldsymbol{\omega}(t))$

It has been assumed throughout the paper that both $\mathbf{R}(t)$ and $\boldsymbol{\omega}(t)$ are known exactly. In practice, these variables may be provided by sensor suites and thus be corrupted by measurement noise. The following theorem addresses the robustness of the proposed filters with respect to disturbances in the rotation matrix $\mathbf{R}(t)$ and the vector $\boldsymbol{\omega}(t)$.

Theorem 3 *Suppose that* $\boldsymbol{\omega}(t)$ *and* $\mathbf{R}(t)$ *are only known up to some error, i.e., the filters operate with* $\boldsymbol{\omega}_m(t) = \boldsymbol{\omega}(t) + \tilde{\boldsymbol{\omega}}(t)$ *and* $\mathbf{R}_m(t) = \tilde{\mathbf{R}}(t)\mathbf{R}(t)$*, with* $\dot{\mathbf{R}}_m(t) = \mathbf{R}_m(t)\mathbf{S}(\boldsymbol{\omega}_m(t))$*, where* $\tilde{\boldsymbol{\omega}}(t)$ *and* $\tilde{\mathbf{R}}(t)$ *parameterize the errors. Further assume that* $\boldsymbol{\eta}(t)$ *remains bounded for all*

t. Then, the estimation errors of both the Kalman and the $\mathcal{H}_\infty$ filters are globally input-to-state stable from the input $\mathbf{U}_m(t) = \left[\|\tilde{\boldsymbol{\omega}}(t)\|, \left\|\tilde{\mathbf{R}}(t) - \mathbf{I}\right\|\right]^T$.

PROOF. In the absence of perturbations, the filter error dynamics are

$$\dot{\tilde{\boldsymbol{\eta}}}(t) = [\boldsymbol{\mathcal{A}}(t) - \boldsymbol{\mathcal{K}}(t)\boldsymbol{\mathcal{C}}(t)]\,\tilde{\boldsymbol{\eta}}(t),$$

where $\boldsymbol{\mathcal{K}}(t)$ is the Kalman or the $\mathcal{H}_\infty$ filter gain. Consider the Lyapunov transformation

$$\tilde{\mathbf{z}}(t) := \mathbf{T}_{cm}^T(t)\mathbf{T}_c(t)\tilde{\boldsymbol{\eta}}(t),$$

where $\tilde{\boldsymbol{\eta}}(t) := \boldsymbol{\eta}(t) - \hat{\boldsymbol{\eta}}(t)$ is the filter error and

$$\mathbf{T}_{cm}(t) := \mathrm{diag}\left(\mathbf{T}_{\mathrm{m}}(\mathrm{t}),\, \mathbf{I},\, \mathbf{I}\right),$$

with $\mathbf{T}_m(t) := \mathrm{diag}\left(\mathbf{R}_{\mathrm{m}}(\mathrm{t}),\, \ldots,\, \mathbf{R}_{\mathrm{m}}(\mathrm{t})\right)$. Let

$$\mathbf{B_s}\left(\boldsymbol{\omega}_m(t)\right) := \mathrm{diag}\left(\mathbf{M}_{\mathrm{s}}\left(\boldsymbol{\omega}_{\mathrm{m}}(\mathrm{t})\right), \mathbf{0}, \mathbf{0}\right)$$

and

$$\boldsymbol{\mathcal{A}}_{cm}(t) := \mathbf{T}_{cm}^T(t)\left[\mathbf{A} - \mathbf{K}(t)\mathbf{C}\right]\mathbf{T}_{cm}(t) - \mathbf{B_s}\left(\boldsymbol{\omega}_m(t)\right),$$

where $\mathbf{K}(t)$ is the Kalman or the $\mathcal{H}_\infty$ filter gain in the LTI space, as previously detailed. The new error dynamics are given by

$$\dot{\tilde{\mathbf{z}}}(t) = \boldsymbol{\mathcal{A}}_{cm}(t)\tilde{\mathbf{z}}(t),$$

which are globally exponentially stable as Lyapunov transformations preserve stability. Thus, there exists a symmetric matrix $\mathbf{X}(t)$ such that

$$\forall_t \;\; c_1\mathbf{I} \preceq \mathbf{X}(t) \preceq c_2\,\mathbf{I},$$

with $c_1, c_2 > 0$, and

$$\forall_t \;\; \boldsymbol{\mathcal{A}}_{cm}^T(t)\mathbf{X}(t) + \mathbf{X}(t)\boldsymbol{\mathcal{A}}_{cm}(t) + \dot{\mathbf{X}}(t) = -\mathbf{I}.$$

It is straigthforward to show that the filter error dynamics in the presence of disturbances in $\boldsymbol{\omega}(t)$ and $\mathbf{R}(t)$ can be written as

$$\begin{aligned}\dot{\tilde{\boldsymbol{\eta}}}(t) = &\boldsymbol{\mathcal{A}}_{cm}(t)\tilde{\boldsymbol{\eta}}(t) + \mathbf{B_s}\left(\tilde{\boldsymbol{\omega}}(t)\right)\boldsymbol{\eta}(t)\\ &+ \left[\mathbf{T}_c^T(t)\mathbf{A}\mathbf{T}_c(t) - \mathbf{T}_{cm}^T(t)\mathbf{A}\mathbf{T}_{cm}(t)\right]\boldsymbol{\eta}(t)\\ &-\mathbf{T}_{cm}^T(t)\mathbf{K}(t)\mathbf{R}_m(t)\left[\boldsymbol{\psi}(t) - \mathbf{R}_m^T(t)\mathbf{C}\mathbf{T}_{cm}(t)\boldsymbol{\eta}(t)\right].\end{aligned}$$

Consider now the Lyapunov-like function

$$V(t) = \tilde{\boldsymbol{\eta}}^T(t)\mathbf{X}(t)\tilde{\boldsymbol{\eta}}(t)$$

and define $K_m := \max\left(\|\mathbf{K}(t)\|\right)$, $L := \max\left(\|\boldsymbol{\eta}(t)\|\right)$, and $\theta \in \mathbb{R}$ such that $0 < \theta < 1$. Then, it is easy to show that

$$\dot{V}(t) \leq -(1-\theta)\,\|\tilde{\boldsymbol{\eta}}(t)\|^2 - \theta\,\|\tilde{\boldsymbol{\eta}}(t)\|\left(\|\tilde{\boldsymbol{\eta}}(t)\| - r\left(\mathbf{U}_m(t)\right)\right),$$

where

$$\begin{aligned}r\left(\|\mathbf{U}_m(t)\|\right) := \frac{2L}{\theta}\,&\left[\|\mathbf{U}_m(t)\|\right.\\ &\left.+ \left(\|\mathbf{A}\| + K_m\,\|\mathbf{C}\|\right)\left[\|\mathbf{U}_m(t)\|^2 + 2\,\|\mathbf{U}_m(t)\|\right]\right].\end{aligned}$$

Thus, it is straightforward to conclude that

$$\dot{V}(t) \leq -(1-\theta)\,\|\tilde{\boldsymbol{\eta}}(t)\|^2 \;\; \forall \|\tilde{\boldsymbol{\eta}}(t)\| > r\left(\mathbf{U}_m(t)\right).$$

As, in addition to that, V satisfies

$$c_1\,\|\tilde{\boldsymbol{\eta}}(t)\|^2 \leq V(t) \leq c_2\,\|\tilde{\boldsymbol{\eta}}(t)\|^2,$$

it follows that the filter error dynamics are globally input-to-state stable from the input $\mathbf{U}_m(t)$.

3.4.3. *Extensions*

The class of systems proposed in Section 3.1 has some constraints that can be lessened, particularly for the system matrices $\mathbf{A}_p$ and $\mathbf{C}_p$. The reader is refered to [4] for further details. Also, although it is not presented in the paper, the optimal smoothing solution, interesting for off-line data processing, is also straightforward to derive following the methodology proposed in the paper. Finally, the problem could have been defined for state variables $\boldsymbol{\eta}_i(t)$ belonging to spaces of different dimensions, e.g., $\boldsymbol{\eta}_i(t) \in X_i \subseteq \mathbb{R}^2, i = 1, \ldots, N$.

4. Simulation Results

To illustrate the performance of the proposed solutions for the estimation of linear motion quantities, a simulation was carried out with the underwater vehicle SIRENE, see [16]. The present case refers to the first problem described in the paper, in Section 2.1, where the AUV is equipped with an USBL, an AHRS, and a DVL. The goal is to estimate the position of a buoy, where an accoustic transponder is installed, and a constant unknown ocean current. Note that, in this case, the position of the transponder that is mounted on the buoy changes with time as the latter, although moored close to the sea surface, may be subject to strong wave action. Nevertheless, the buoy wave induced random motion can be modeled as an external disturbance acting on the USBL positioning system, and its description embedded in the frequency weights as presented in Section 3. In addition to the disturbances induced by the ocean waves, sensor noise was added to all sensors. In particular, additive zero-mean white Gaussian noise was considered, with standard deviation of 1 m for the USBL and 0.01 m/s for the velocity measurements relative to the water. The AHRS was assumed to provide the roll, pitch, and yaw Euler angles, also corrupted by additive zero-mean white Gaussian noises with standard deviation of 0.05 ° for the roll and pitch and 0.5 ° for the yaw, and the angular velocity corrupted with white Gaussian noise with standard deviation of 0.02 °/s. The filter design should not only reject the wave induced disturbances from the position measurements to the position and current velocity estimates, but also the noise in the position and relative velocity measurements.

The disturbances induced by the three-dimensional wave random field in the position of the buoy are modeled using three second-order harmonic oscillators representing the disturbance models along the x, y, and z directions,

$$H_w^i(s) = \frac{\sigma_i s}{s^2 + 2\xi_i\omega_{0i}s + \omega_{0i}^2},\; i = 1,\, 2,\, 3,$$

where ω_{0i} is the dominating wave frequency along each axis, ξ_i is the relative damping ratio, and σ_i is a parameter related to the wave intensity, see [6] for further details. The sensor frequency weight matrix transfer function $\mathbf{W}_n(s)$ was chosen as

$$\mathbf{W}_n(s) = \left(1 + \frac{\sigma_i s}{s^2 + 2\xi_i\omega_{0i}s + \omega_{0i}^2}\right)\mathbf{I}_3.$$

Notice that a direct term was included, not only to satisfy design requirements (nonzero sensor noise), but also to model the noise on the USBL, . In the simulation the dominating wave frequency was set to $\omega_{0i} = 0.8975\text{rad/s}$ and the relative damping ratio to $\xi_i = 0.1$. The system disturbance weight transfer matrix was chosen as $\mathbf{W}_d(s) = 0.01\mathbf{I}_6$. The filter initial states were chosen to reflect the knowledge of the position of the transponder as given by the USBL sensor.

Albeit it was not explicitly shown, the Kalman filter error dynamics have an equivalent LTI description that relates to the LTV dynamics through the transformation matrix $\mathbf{T}_c(t)$, which preserves the norm of the different state estimation errors and only affects the directionality over time. Figure 2 shows the singular values of the linear time invariant closed-loop transfer functions from the disturbances and sensor noise input, $\mathbf{d}$ and $\mathbf{n}$, respectively, to the position and current velocity estimate errors, in the inertial frame, of the Kalman filter. The diagram shows that the performance requirements are met by the resultant filter, which is evident from the band rejection characteristics of the notch present in the diagram.

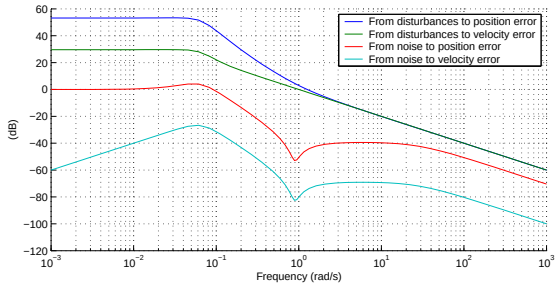

Fig. 2. Singular values of the Kalman LTI filter error dynamics

Finally, it is important to remark that the proposed solution results in a complimentary filter. Indeed, it is easy to show that, in the frequency domain,

$$\hat{\mathbf{E}}(s) = \frac{F_1(s)\mathbf{U}(s) + F_2(s)\mathbf{E}(s)}{sF_1(s) + F_2(s)},$$

where $\mathbf{E}$ stands for the frequency representation of the position of the buoy in the LTI space, $\hat{\mathbf{E}}$ its estimate, and $\mathbf{U}$ the system input in LTI coordinates. Since $\mathbf{U}(s) = s\mathbf{E}(s)$ it follows that $\hat{\mathbf{E}}(s) = \mathbf{E}(s)$. Thus, low-band position signals are combined with high-band velocity readings to achieve a complimentary filter.

The trajectory described by the vehicle is shown in Fig. 3, where the undisturbed position of the buoy is marked with a cross. The actual position of the buoy, expressed in inertial frame coordinates, is depicted in Fig. 4. As it can be seen, the buoy wave induced random motion is confined to an interval of about 10 m of height, which corresponds to extreme weather conditions.

The evolution of the filter error variables is shown in Fig. 5. The initial transients arise due to the mismatch of the initial conditions of the states of the filter and can be considered as a warming up time of 180 s of the corresponding

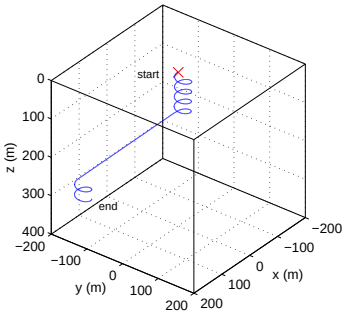

Fig. 3. Trajectory described by the vehicle

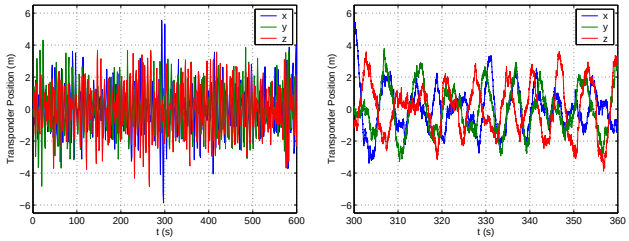

(a) Overall (b) Zoom

Fig. 4. Time evolution of the position of the buoy (expressed in inertial coordinates)

Integrated Navigation System. The filter error variables are shown in greater detail in Fig. 6. From the various plots it can be concluded that the disturbances induced by the waves, as well as the noise of the sensors, are highly attenuated by the filter, producing very accurate estimates of the velocity of the current and the position of the buoy.

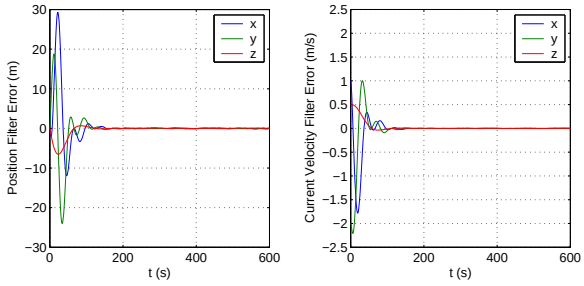

Fig. 5. Time evolution of the Kalman filter error variables

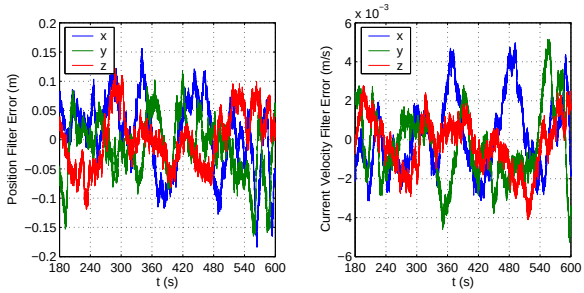

Fig. 6. Detailed evolution of the Kalman filter error variables

It should be said that the proposed solution for the estimation of the position and the velocity of the ocean current

is optimal with respect to disturbances arising from all sensors but the Attitude and Heading Reference System. This is reflected in the performance exhibited by the proposed filter, as the simulation results clearly demonstrate. Also, if a faster convergence rate is required, a simple gain switching technique may be employed, enabling a very fast convergence during startup and optimal filtering performance afterwards.

Finally, it is shown a comparison between the proposed filter and the traditional solution, which consists in transforming all the data into inertial coordinates and then apply the classical LTI Kalman filter. This is strongly undesirable as the effect of the noise on the attitude of the vehicle, essential for the transformation into inertial coordinates, may be greatly amplified in the filter estimates, particularly when the vehicle is farther from the transponder. The steady-state standard deviation of the errors for both strategies are given in Table 1. The differences between both strategies are notorious and clearly demonstrate the improved performance obtained with the proposed solution.

Table 1
Standard deviation of the filter errors

Standard deviation of of the errors	Proposed Filter	Inertial Filter
Position - x axis (m)	0.063	1.27
Position - y axis (m)	0.051	1.05
Position - z axis (m)	0.047	0.17
Velocity - x axis (cm/s)	0.186	1.63
Velocity - y axis (cm/s)	0.187	1.08
Velocity - z axis (cm/s)	0.132	0.223

5. Conclusions

Navigation Systems are a key component in the design of a great variety of vehicular applications. This paper presented the design and performance evaluation of a set of globally stable time-varying optimal kinematic filters with applications to the estimation of linear motion quantities of mobile platforms (position, linear velocity, ocean current velocity, and acceleration) in three dimensions. The proposed solutions are based on the Kalman and $\mathcal{H}_\infty$ optimal filters for linear time-varying systems and the explicit optimal filtering solutions are obtained through the use of an appropriate coordinate transformation, whereas the design employs frequency weights to achieve adequate disturbance rejection and attenuation of the measurement noise on the state estimates. Two examples of application in the field of ocean robotics were presented that demonstrate the potential and usefulness of the proposed design methodology. In the first a navigation filter is designed for the estimation of unknown constant ocean currents. In the second case the proposed solution addresses the problem of estimation of the velocity of an underwater vehicle, as well as the acceleration of gravity. Both solutions result in complimentary filters and simulation results were shown for the first that illustrate the filtering achievable performance in the presence of both extreme environmental disturbances and realistic measurement noise. A comparison with traditional techniques developed in inertial coordinates is also shown which evidenced the benefits of this new solution.

References

[1] A. Gelb (Ed). *Applied Optimal Filtering*. The MIT Press, 1974.

[2] B. Anderson and J. Moore. *Optimal Filtering*. Dover Publications, 1995.

[3] P. Batista, C. Silvestre, and P. Oliveira. A Quaternion Sensor Based Controller for Homing of Underactuated AUVs. In *Proc. 45th IEEE Conference on Decision and Control*, pages 51–56, San Diego, USA, December 2006.

[4] P. Batista, C. Silvestre, and P. Oliveira. Kalman and $\mathcal{H}_\infty$ Optimal Filtering for a Class of Kinematic Systems. In *Proc. 17th IFAC World Congress*, Seoul, Korea, July 2008.

[5] Roger W. Brockett. *Finite Dimensional Linear Systems*. Wiley, 1970.

[6] T. I. Fossen and J. P. Strand. Passive nonlinear observer design for ships using Lyapunov methods: full-scale experiments with a supply vessel. *Automatica*, 35(1):3–16, January 1999.

[7] T.I Fossen and A. Grøvlen. Nonlinear Output Feedback Control of Dynamically Positioned Ships Using Vectorial Observer Backstepping. *IEEE Trans. on Control Systems Technology*, 6(1):121–128, January 1998.

[8] H. Nijmeijer and T. I. Fossen (Eds). *New Directions in Nonlinear Observer Design (Lecture Notes in Control and Information Sciences)*. Springer, 1999.

[9] J. C. Kinsey, R. M. Eustice, and L. L. Whitcomb. A Survey of Underwater Vehicle Navigation: Recent Advances and New Challenges. In *Proc. 7th IFAC Conference on Manoeuvring and Control of Marine Craft (MCMC2006)*, Lisboa, Portugal, September 2006.

[10] K. Nagpal and P. Khargonekar. Filtering and Smoothing in an $\mathcal{H}_\infty$ Setting. *IEEE Trans. on Automatic Control*, 36(2):152–166, February 1991.

[11] C. Nguyen and T. Lee. Design of a State Estimator for a Class of Time-Varying Multivariable Systems. *IEEE Trans. on Automatic Control*, 30(2):179–182, February 1985.

[12] A. Pascoal, I. Kaminer, and P. Oliveira. Navigation System Design Using Time Varying Complementary Filters. *IEEE Aerospace and Electronic Systems*, 36(4):1099–1114, October 2000.

[13] J. E. Refsnes, A.J. Sørensen, and K. Y. Pettersen. Robust observer design for underwater vehicles. In *Proc. 46th IEEE Conf. on Control Applications*, Munich, Germany, October 2006.

[14] A. Robertsson and R. Johansson. Comments on Nonlinear Output Feedback Control of Dynamically Positioned Ships Using Vectorial Observer Backstepping. *IEEE Trans. on Control Systems Technology*, 6(3):439–441, May 1998.

[15] P. G. Savage. Strapdown Inertial Navigation Integration Algorithm Design Part 2: Velocity and Position Algorithms. *Journal of Guidance, Control, and Dynamics*, 21(2):208–221, March 1998.

[16] C. Silvestre, A. Aguiar, P. Oliveira, and A. Pascoal. Control of the SIRENE Underwater Shuttle: System Design and Tests at Sea. In *Proc. 17th International Conference on Offshore Mechanics and Artic Engineering (OMAE'98- Conference)*, July 1998.